J Supercond Nov Magn (2015) 28:3267–3273
DOI 10.1007/s10948-015-3193-4

ORIGINAL PAPER

Charge Transfer Mechanism and Superconductivity in $Tl_{0.5}Cu_{0.5}$ $(Ba_{1-x}Sr_x)Ca_2Cu_3O_y$ ($x = 0$, 0.15,0.25,0.35) Samples

Nawazish A. Khan[1] · **M. Husnain Zeb**[1]

Received: 15 May 2015 / Accepted: 23 July 2015 / Published online: 13 August 2015

Abstract $Tl_{0.5}Cu_{0.5}(Ba_{1-x}Sr_x)Ca_2Cu_3O_y$ ($x = 0$, 0.15,0.25,0.35) superconductors are prepared by a two-step solid-state reaction method, and their superconducting properties are studied by resistivity, susceptibility, FTIR, XRD, and excess conductivity analyses. The samples have shown an orthorhombic crystal structure in which the c-axis length and the volume of the unit cell increase with Sr doping. The normal-state resistivity is appreciably suppressed, and the zero resistivity critical temperature observed between 97 and 104 K. The magnitude of the superconductivity is enhanced in Sr-doped samples. In the Fourier transform infrared (FTIR) absorption measurements, the apical oxygen phonon mode is observed to be softened with Sr doping whereas the peak position of planar oxygen stays unaltered in Sr-incorporated samples. The excess conductivity analyses of $Tl_{0.5}Cu_{0.5}(Ba_{1-x}Sr_x)Ca_2Cu_3O_y$ ($x = 0$, 0.15,0.25,0.35) samples have shown that the values of $\xi_{c(0)}$, the inter-layer coupling J, are not appreciably altered whereas the Fermi velocity v_F of superconducting carriers and the phase relaxation increase with Sr doping. The values of parameters such as $B_{c0}(T)$, $B_{c1}(T)$, $J_c(0)$ are, however, enhanced with the doping of Sr in the final compound. These studies have shown that Sr doping promotes efficient transfer of the carriers from charge reservoir layer to the conducting CuO_2 planes thereby promoting enhancement in the density of carriers and hence increase in the values of aforementioned superconductivity parameters.

Keywords $Tl_{0.5}Cu_{0.5}(Ba_{1-x}Sr_x)Ca_2Cu_3O_y$ superconductors · Charge transfer mechanism · Softening of apical oxygen modes · Enhancement of $B_{c0}(T)$ · $B_{c1}(T)$ · $J_c(0)$

1 Introduction

The crystal chemistry of cuprate high-temperature superconductors consists of a charge reservoir layer and number conducting CuO_2 planes which are separated by Ca atoms. The role of the charge reservoir layer is to supply the carriers to the conducting planes whereas the superconductivity lies in CuO_2 planes. The Ca atoms develop inter-plane coupling. We have extensively investigated the role of Ca atoms in developing inter-plane coupling by doping Be and Mg at the Ca sites [1, 2]. In the previous studies, we have observed that the partial substitution of Be and Mg at Ca sites resulted in a decrease in the c-axes length that provided direct evidence of increased inter-plane coupling. The enhancement of the inter-plane coupling is bought about by the small atomic size of the doped Be and Mg atoms at Ca sites. The enhancement of inter-plane coupling resulted into an increase in the $T_c(R = 0)$ and magnitude of diamagnetism of $Cu_{0.5}Tl_{0.5}Ba_2Ca_{n-1}Cu_nO_{2n+4-\delta}$ ($n =$ 2,3,4,5) superconductors. Those studies confirmed the pivotal role of inter-plane coupling in the mechanism of high T_c superconductors. In the current findings, we have tried to decrease the thickness of the $Cu_{0.5}Tl_{0.5}Ba_2O_{4-\delta}$ charge reservoir layer by doping Sr(2.15 Å) at the Ba(2.21 Å) sites. The thickness of $Cu_{0.5}Tl_{0.5}Ba_2O_{4-\delta}$ charge reservoir layer is 4.2 Å whereas the thickness of superconducting blocks

✉ Nawazish A. Khan
Nakhan@Qau.Edu.Pk

[1] Materials Science Laboratory, Department of Physics, Quaid-i-Azam University, Islamabad 45320, Pakistan

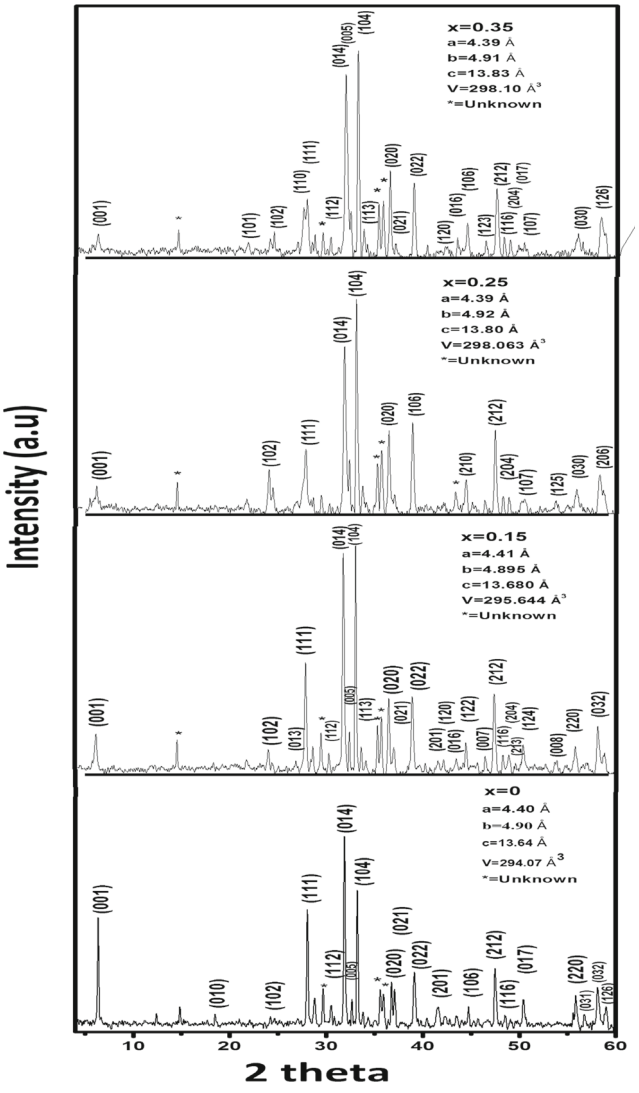

Fig. 1 Xrd scans of $Tl_{0.5}Cu_{0.5}(Ba_{1-x}Sr_x)Ca_2Cu_3Oy$ ($x = 0$, 0.15, 0.25, 0.35)

containing a Ca atom at their center is 3.2 Å. The decrease in the thickness of the charge reservoir layer in current studies is brought about by doping a smaller sized Sr at the Ba sites. The effect of doped Sr atoms at the intrinsic superconductivity parameters is investigated by carrying excess conductivity analysis of conductivity data.

In previous studies, Sr-doped $Tl_{0.6}Pb_{0.4}Ba_{2-x}Sr_xCa_2Cu_3O_{9-\delta}$ (x= 0,0.10,0.20,0.30,0.40,0.50) samples were synthesized by a two-step solid-state reaction method [1]. Highest zero resistivity temperature was observed at 113 K for $x = 0.5$, and their X-ray diffraction (XRD) analysis showed a pseudo-tetragonal structure. Increase in c-axis lattice constant with the Sr content was observed. In another study, Sr-doped $Y(Ba_{2-y}Sr_y)Cu_3O_{6+\delta}$ superconductors were prepared by a two-step solid-state reaction method at 950 °C [2]. In order to optimize the density of carriers, the samples were annealed in a flowing O_2 environment for 20 h. An XRD scan of the annealed samples had shown an orthorhombic structure with zero resistivity temperature at 90 K for $y = 0$ and 84 K for $y = 0.8$ content of Sr. They had observed that chemical substitution of Sr^{2+} ions in fully oxygenated samples leads to a decrease in T_c. Sr-doped $YBa_{2(1-x)}Sr_xTh_xCu_3O_{7-\delta}$ ($x = 0.1$,0.15.0.2 and 0.3) superconductors were prepared at 850° [3]. The XRD scans had shown that double-doped 123 superconductors have mainly single-phase orthorhombic crystal structure with some small extra peaks attributed to secondary phases like tetragonal and non-superconducting YBCO and $Y_2Cu_2O_5$ phases. The replacement of Ba by Sr had caused a distortion in the perovskite structure and brought shrinking in three axes. Moreover, the orthorhombic splitting of the lattice parameters was also affected by Sr content and was correlated to a decrease in T_c. Sr-doped $Hg_2(Ba_{1-y}Sr_y)_2YCu_2O_{8-\delta}$ superconductors were synthesized at high pressure (3.5–4 GPa) and temperature (900–1050°) [4]. An increase in T_c was observed with an increase in "y" which reached 42 K for $y = 1.0$. The main phase was Hg-2212, but sometimes for Sr-rich compositions, Hg-1212 impurity phase was observed due to some reaction with gold capsule enhanced by Sr content. A decrease in "a" and "c" axis lengths was observed with an increase in Sr content. The structure of Hg-2212 belonged to space group I/4mmm. Sr-doped samples of $La_{2-x}Sr_xCuO_4$ superconductors were prepared under high pressure up to 20 kbar [5]. They observed that T_o decreases with pressure. The T_c of the samples for $x \leq 0.206$ increases with the pressure until a critical pressure P_c, but pressure dependence of T_c becomes very small above P_c. Sr-doped samples of $Ba_2Ca_{2+x}Cu_{3+y}O_z$ ($T_c = 126$ K) superconductors were prepared under 5 GPa at 800–950° [6]. A slight decrease up to ~ 121 K was observed due to Sr doping. With increased Sr concentration more than 0.40, a new superconducting phase was observed with $T_c \sim 106$ K. The cation composition was (Ba + Sr)/Ca/Cu ~ 2:1:2, and it was indexed with I4 symmetry with lattice constants "$a = 3.86$ Å" and "c = 22 Å." A series of compounds having compositions $(Er_{0.76}Ca_{0.24})Ba_{2-y}Sr_y(Cu_{2.76}Co_{0.24})O_z$ ($y = 0.0$,0.2,0.4,0.6) and $(Er_{1-x}Ca_x)Ba_{1.4}Sr_{0.6}(Cu_{2.76}Co_{0.24})O_z$ ($x = 0.24$,0.36,0.48) were prepared by a standard ceramic technique [7]. The XRD pattern showed that three Sr-doped samples ($y = 0.0$–0.6) remained orthorhombic, while two Ca-Sr doped samples ($x = 0.36$ and 0.48, $y = 0.6$) approached tetragonal structure. The XRD pattern revealed that Sr-doped Y-123 showed a decrease of the unit cell volume. A decrease in T_c and oxygen content was observed with an increase in Sr content. The suppression in the T_c and oxygen content was attributed to the arrangement of oxygen atoms in the basal plane. B.R. Hickey et al. prepared Sr-doped $(La_{1-x}Sr_x)OFeAs$ ($x = 0.10$–0.30) and $La(O_{0.9}$

Table 1 Susceptibility combined graph of $Tl_{0.5}Cu_{0.5}(Ba_{1-x}Sr_x)Ca_2Cu_3O_y$ (x = 0, 0.15, 0.25, 0.35)

Sample	Resistivity (as-prepared)		Susceptibility (as-prepared)		Lattice parameters from XRD			
	T_c ($R = 0$), K	T_c (onset), K	M.D	T_c (onset), K	a (Å)	b (Å)	c (Å)	d (Å)
$X = 0$	97	113	0.08	110	4.4	4.9	13.64	294.078
$X = 0.15$	102	112	0.9	108	4.39	4.89	13.68	295.644
$X = 0.25$	96	113	0.11	99	4.39	4.92	13.68	298.063
$X = 0.35$	104	113	0.12	103	4.39	4.91	13.85	298.535

$F_{0.1-\delta}$)FeAs samples by a two-step method [8]. It was revealed from the XRD analysis that all samples gave clear evidence that the main peaks were from $(La_{1-x}Sr_x)$OFeAs phase. All main peaks could be indexed by a tetragonal structure with lattice parameters "$a = b = 4.035$ Å" and "$c = 8.7710$ Å." These cell parameters are a bit larger than those in parent phase LaOFeAs ($a = b = 4.032$ Å and $c = 8.726$ Å) which suggested that lattice expanded a bit with Sr substitution. Resistivity measurements showed that the maximum transition temperature was about 25 K at a doping level of $x = 0.13$ and no superconductivity was observed beyond $x = 0.23$. Sr-doped $Sr_{2-x}Ba_xCuO_{3+\delta}$ ($x \leq 0.6$) superconductors were synthesized under a high pressure of 6 GPa at 1000 °C [9]. Maximum T_c was obtained in the undoped $SrCuO_{3+\delta}$ sample. The XRD analysis was done, and it was found that for $x \leq 0.6$, apparently all the samples were tetragonal single phase and belonged to space group I4/mmm. Single-phase superconducting samples of $(Bi/Pb)_2(Sr_{2-x}Ca_x)_2Cu_3O_{10}$ were synthesized a by solid-state reaction method [10]. DC electrical resistivity were carried out, and it was found that a prepared sample with $x = 0.6$, with optimally nominal oxygen content (over doped), showed T_c of 107 K. The XRD analysis has shown that crystal belonged to a tetragonal system and had a space group of I4/mmm.

2 Experimental

The $Tl_{0.5}Cu_{0.5}(Ba_{1-x}Sr_x)Ca_2Cu_3O_y$ ($x = 0$, 0.15, 0.25, 0.35) samples were prepared using a solid-state reaction method. We started out with the precursor material of non-stoichiometric composition of form $Tl_{0.5}Cu_{0.5}(Ba_{1-x}Sr_x)Ca_2Cu_3O_y$ ($x = 0$, 0.15, 0.25, 0.35) and used $Ba(NO_3)_2$, $Ca(NO_3)_2$, $SrCO_3$, and Cu(CN) as starting compounds. These materials were mixed for 1 h and fired twice at 860 °C in quartz boat for 24 h. The precursor material after firing was mixed with Tl_2O_3 to give $Tl_{0.5}$ $Cu_{0.5}(Ba_{1-x}Sr_x)Ca_2Cu_3O_y$ ($x = 0$, 0.15, 0.25, 0.35) as a final reactant composition. Thallium-mixed material was pressed under a pressure of 3.8 tons/cm^2 to make disc-shaped pallets. These pallets were enclosed in a gold capsule and sintered at 860 °C for 10 min. The samples were characterized by resistivity, ac susceptibility, and Fourier transform infrared spectroscopic measurements. The FTIR absorption measurements were carried out by using a Nicolet 5700 Fourier transform infrared spectrometer (FTIR) in 400–700 cm^{-1} wave number range. The crystal structure of

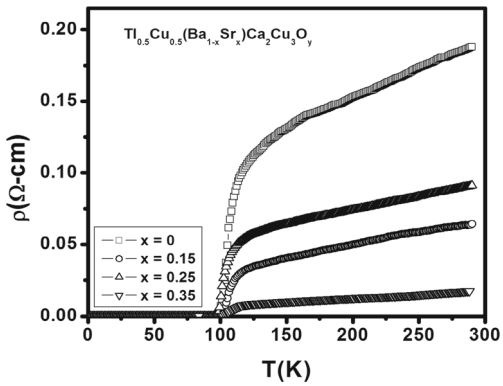

Fig. 2 Resistivity vs temperature combined graph of $Tl_{0.5}Cu_{0.5}(Ba_{1-x}Sr_x)Ca_2Cu_3Oy$

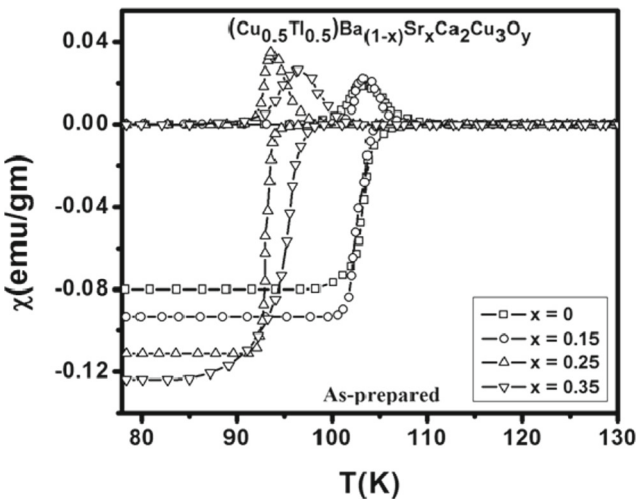

Fig. 3 Susceptibility combined graph of $Tl_{0.5}Cu_{0.5}(Ba_{1-x}Sr_x)$ Ca_2Cu_3Oy (x = 0, 0.15, 0.25, 0.35)

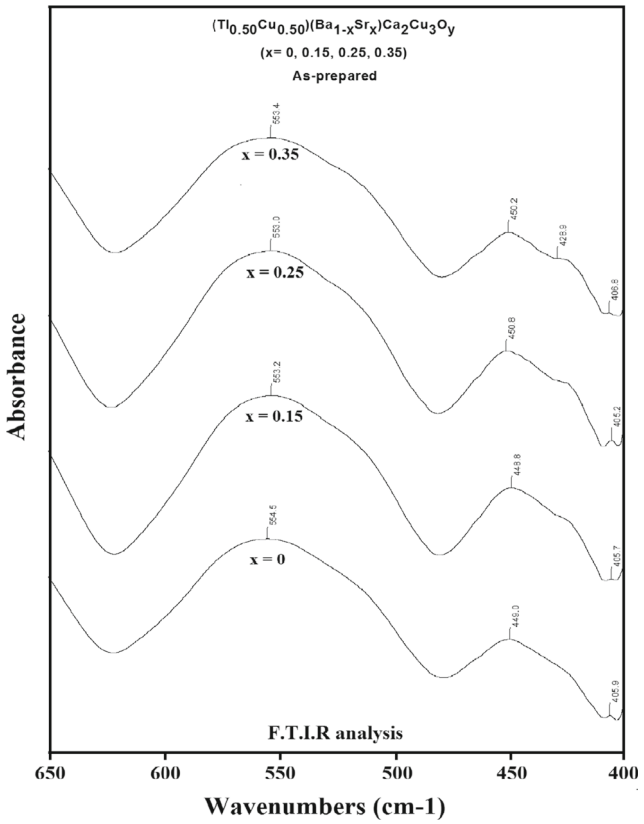

Fig. 4 FTIR spectra for $Tl_{0.5}Cu_{0.5}(Ba_{1-x}Sr_x)Ca_2Cu_3O_y$ ($x = 0$, 0.15, 0.25, 0.35)

the samples was measured by X-ray diffraction scan using Bruker DX 8 Focus employing CuKα radiations of wavelength 1.54056 Å. The cell parameters were determined by check cell computer refinement program. The oxygen content in the final compound was optimized by carrying out post-annealing of the samples for 6 h in a tubular furnace in flowing oxygen atmosphere at 500°.

3 Results and Discussion

The X-ray diffraction scans of $Tl_{0.5}Cu_{0.5}(Ba_{1-x}Sr_x)Ca_2Cu_3O_y$ ($x = 0$, 0.15, 0.25, 0.35) samples are shown in Fig. 1. Most of the diffraction lines are fitted to the orthorhombic crystal structure by following PMMM space group. The c-axis length and the volume of the unit cell of $Tl_{0.5}Cu_{0.5}(Ba_{1-x}Sr_x)Ca_2Cu_3O_y$ ($x = 0$, 0.15, 0.25, 0.35) samples increase with increased Sr content (Table 1). It is most likely that smaller sized Sr promotes relaxation of the lattice axes that would likely result into an increase in the thickness of the charge reservoir layer. The resistivity versus temperature measurements of $Tl_{0.5}Cu_{0.5}(Ba_{1-x}Sr_x)Ca_2Cu_3O_y$ ($x = 0$, 0.15, 0.25, 0.35) samples are displayed in Fig. 2. All the samples have shown metallic variations of resistivity from the room temperature down to onset of superconductivity. The room temperature resistivity is significantly reduced with increased Sr doping which shows that Sr incorporation induces a more metallic character in the final compound. $Tl_{0.5}Cu_{0.5}(Ba_{1-x}Sr_x)Cu_3O_y$ ($x = 0$, 0.15, 0.25, 0.35) samples are shown onset of superconductivity around 113, 112, 113, and 113 K and $T_c(R = 0)$ at 97, 102, 96, and 104 K, respectively. The AC magnetic susceptibility measurements of $Tl_{0.5}Cu_{0.5}(Ba_{1-x}Sr_x)Ca_2Cu_3O_y$ ($x = 0$, 0.15, 0.25, 0.35) samples are shown in Fig. 3. The onset of superconductivity in these samples is observed around 110, 108, 99, and 103 K (Table 1). The magnitude of diamagnetism systematically increases with Sr doping.

The FTIR absorption measurements of $Tl_{0.5}Cu_{0.5}(Ba_{1-x}Sr_x)Ca_2Cu_3O_y$ ($x = 0$, 0.15, 0.25, 0.35) samples are shown in Fig. 4. In the phonon spectra of these samples, three prominent absorption modes related to the vibrations of oxygen atoms are observed around 450, 555, and 570 cm^{-1}. The former two modes are related to the vibrations of apical oxygen atoms whereas the last mode to the vibrations of CuO_2 planar oxygen atoms. The former apical oxygen mode is slightly hardened whereas the later mode is softened (by 2 cm^{-1}). The third mode stays almost unchanged at around 570 cm^{-1}. The main route cause of this hardening/softening of apical oxygen modes is incorporation of Sr at the charge reservoir layer. The effect of Sr doping at the Ba sites on the intrinsic superconductivity parameters has also been investigated by carrying out excess conductivity analysis (FIC) of conductivity data of $Tl_{0.5}Cu_{0.5}(Ba_{1-x}Sr_x)Ca_2Cu_3O_y$ ($y = 0$, 0.15, 0.25, 0.35) samples.

Table 2 Widths of critical, 3D, 2D, and 0D fluctuation regions observed from fitting of the experimental data of $Tl_{0.5}Cu_{0.5}(Ba_{1-x}Sr_x)Ca_2Cu_3O_y$ ($x = 0$, 0.15, 0.25, and 0.35) samples using AL model0

Sample	λ_{CR}	λ_{3D}	λ_{2D}	λ_{SW}	$T_{CR-3D} = T_G$ (K)	T_{3D-2D} (K)	T_{2D-SW} (K)	T_{CMF}	T^* (K)	$\alpha = \rho_n(0\ K)(\Omega-cm)$	$W = \Delta T_c$ (K)
0	–	0.50	1.01	2.03	102.3	103.4	111.4	101.3	138.5	0.717	7.97
0.15	–	0.53	1.00	2.02	104.4	105.4	108.4	103.4	122.4	0.011	4.88
0.25	0.29	0.49	0.99	2.01	103.3	104.4	108.5	102.4	119.4	0.036	4.75
0.35	–	0.54	1.00	2.02	105.4	106.4	108.4	104.4	113.4	0.002	1.93

Table 3 The superconductivity parameters observed from the FIC analysis of $Tl_{0.5}Cu_{0.5}(Ba_{x1-x}Sr_x)Ca_2Cu_3O_y$ (x = 0, 0.15, 0.25, and 0.35) superconductors

Sample	ξ_c (0) (Å)	J	N_G	$\lambda_{p.d}$ (Å)	Bc(0) (T)	B_{c1} (T)	B_{c2} (T)	κ	Jc(0)*10^3 (A/cm^2)	V_F*10^7 (ms)	E_{Break}	τ_φ*10^{-14}
0	0.975	0.019	0.073	304.1	4.78	0.52	128.7	19.0	8.56	0.79	0.025	16.0
0.15	0.988	0.019	0.019	215.1	6.76	0.92	128.7	13.45	17.09	0.86	0.008	47.2
0.25	0.95	0.019	0.072	288.9	5.04	0.57	128.7	18.05	9.49	0.78	0.018	22.1
0.35	0.971	0.019	0.013	190.8	7.62	1.12	128.7	11.92	21.73	0.86	0.006	64.9

3.1 Excess Conductivity Analyses (FIC) of $Tl_{0.5}Cu_{0.5}(Ba_{1-x}Sr_x)Ca_2Cu_3O_y$ ($x = 0, 0.15, 0.25, 0.35$) Samples

The excess conductivity analyses accomplished by using the equation $\Delta\sigma_{(T)} = \Delta\sigma_{RT}\varepsilon^{-\lambda D}$ in the temperature regime around T_c and beyond. This equation can be written in the form as follows:

$$\ln\Delta\sigma_{(T)} = \ln\Delta\sigma_{RT} - \lambda_D \ln(\varepsilon) \quad (1)$$

where $\varepsilon = \left[\frac{T - T_c^{mf}}{T_c^{mf}}\right]$ is the reduced temperature and λ_D is the dimensional exponent. The dimensional exponent has values 0.3, 0.5, 1.0, and 2.0 for critical, three-dimensional (3D), two-dimensional (2D), and zero-dimensional (0D) conductivities, respectively [13–15]. The Lawrence and Doniach (LD) model used for the analyses of the polycrystalline samples is of the form [16]

$$\Delta\sigma_{LD} = [e^2/(16\hbar d)](1 + J\varepsilon^{-1})^{-1/2}\varepsilon^{-1} \quad (2)$$

Here, $J = \{2\xi_{c(0)}/d\}^2$ is the inter-layer coupling and d as the thickness of superconducting layers (∼ 15 Å in current studies) and $\xi_{c(0)}$ is the coherence length along the c-axis. We have determined various crossover temperatures, such as T_G, T_{3D-2D}, and T_{2D-0D}, from the log plot of the excess conductivity versus the reduced temperature, see Tables 2 and 3. These crossover temperatures are determined from the intersection of various dimensional exponents, i.e., λ_{cr} refers to the slope below T_G, λ_{3D} above

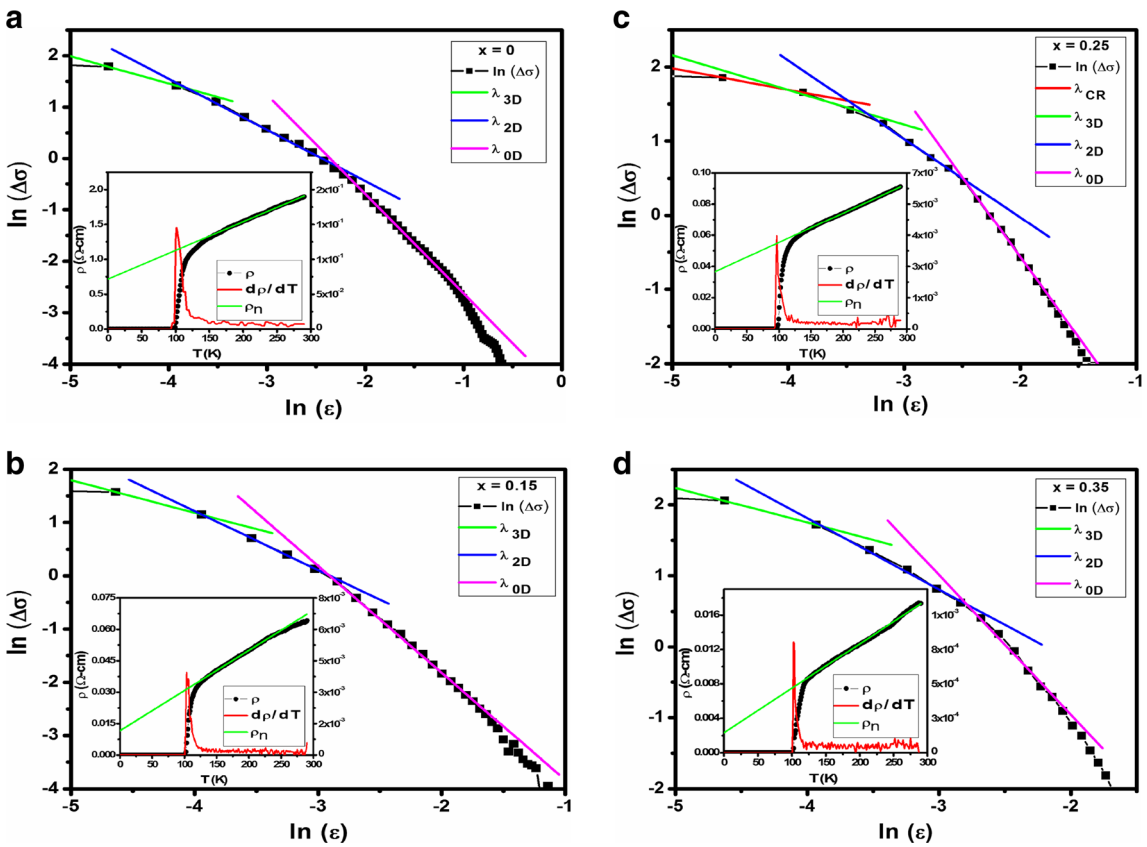

Fig. 5 **a** $\ln(\Delta\sigma)$ vs $\ln(\varepsilon)$ of $Tl_{0.5}Cu_{0.5}(Ba_{1-x}Sr_x)Ca_2Cu_3O_y$ for $x = 0$. **b** $\ln(\Delta\sigma)$ vs $\ln(\varepsilon)$ of $Tl_{0.5}Cu_{0.5}(Ba_{1-x}Sr_x)Ca_2Cu_3O_y$ for $x = 0.15$. **c** $\ln(\Delta\sigma)$ vs $\ln(\varepsilon)$ of $Tl_{0.5}Cu_{0.5}(Ba_{1-x}Sr_x)Ca_2Cu_3O_y$ for $x = 0.25$. d $\ln(\Delta\sigma)$ vs $\ln(\varepsilon)$ of $Tl_{0.5}Cu_{0.5}(Ba_{1-x}Sr_x)Ca_2Cu_3O_y$ for $x = 0.35$

T_G, and λ_{2D} to the slope value above T_{3D-2D} and λ_{0D} corresponds to the slope of exponent value 2, respectively, Fig. 5a–d. The parameters such as $\xi_{c(0)}$, the inter-layer coupling J are not appreciably altered whereas the Fermi velocity v_F of superconducting carriers and their phase relaxation time are enhanced with the doping of Sr in the final compound.

The Ginzburg number N_G in the transition region and the temperature T_G are determined from the intersection of critical and three-dimensional regimes. By employing the T_G and the N_G and using the Ginzburg-Landau theory, important superconducting parameters are determined by using the following equations [17–19]:

$$N_G = \left| \frac{T_G - T_c^{mf}}{T_c^{mf}} \right| = 0.5[K_B T_c / B_{c(0)}^2 \gamma^2 \xi_{c(0)}^3]^2 \quad (3)$$

$$B_c = \frac{\Phi_0}{2\sqrt{2}\pi \lambda_{p.d(0)} \xi_{ab(0)}} \quad (4)$$

$$B_{c1} = \frac{B_c}{\kappa\sqrt{2}} \ln \kappa \quad (5)$$

$$B_{c2} = \sqrt{2}\kappa B_c \quad (6)$$

$$J_c = \frac{4\kappa B_{c1}}{3\sqrt{3}\lambda_{p.d(0)} \ln \kappa} \quad (7)$$

T_c^{mf} is the mean field critical temperature and is determined from the point of inflection of the temperature of derivative of resistivity ($d\rho/dT$). The Ginzburg-Landau (GL) parameter is defined as $\kappa = \lambda/\xi$. The phase relaxation time of the Cooper pair is calculated by using the following equation [20]:

$$\tau_\varphi = \frac{\pi\hbar}{8k_B T \varepsilon_0} \quad (8)$$

The coupling constant [$\lambda = \frac{\hbar\tau_\varphi^{-1}}{2\pi k_B T}$] is determined by using the phase relaxation time τ_ϕ. The Fermi velocity of the carriers and the energy required to break apart the Cooper pairs are determined by using the following expressions; the value of the proportionality coefficient $K \cong 0.12$ is used as in reference [17].

$$V_F = \frac{5\pi k_B T_c \xi_{c(0)}}{2\hbar} \quad (9)$$

$$E = \frac{h}{\tau_\varphi (1.6 \times 10^{-19})} (eV) \quad (10)$$

By using N_G values in the critical regime of $Tl_{0.5}Cu_{0.5}(Ba_{1-x}Sr_x)Ca_2Cu_3O_y$ ($x = 0, 0.15, 0.25, 0.35$) samples, the $B_{c(0)}$, $B_{c1(0)}$, $B_{c2(0)}$, $J_c(0)$, and $\kappa = \lambda/\xi$ are determined by using the aforementioned equations [10–12]. The values of $B_{c0}(T)$, $B_{c1}(T)$, and $J_c(0)$ are enhanced with the increased Sr doping (Table 2). The thermodynamic critical field B_c is related to the free energy difference between the normal and superconducting electrons. The increase in the values of these parameters suggests that efficient transfer of the mobile charge carrier takes place which increases the Cooper pair density in the conducting CuO_2 planes. Moreover, it is most likely that the flux pinning characters is enhanced with Sr doping in the final compound. The energy required to break the Cooper pairs apart into normal electrons, the magnetic field penetration depth $\lambda_{p.d}$, and the Ginzburg-Landau (GL) parameter κ are suppressed with Sr incorporation. The phase relaxation time of the carriers increases with Sr doping.

4 Conclusion

Sr-doped $Tl_{0.5}Cu_{0.5}(Ba_{1-x}Sr_x)Ca_2Cu_3O_y$ ($x = 0, 0.15, 0.25, 0.35$) superconducting samples are synthesized at a normal pressure, and their superconducting properties are determined. A significant decrease in the room temperature resistivity is observed with the doping of Sr. All the samples have shown metallic variations of resistivity and zero resistivity critical temperature ranging from 97 to 104 K. Magnitude of the superconductivity is significantly enhanced with the doping of Sr in the final compound. The phonon modes related to vibrations of apical oxygen atoms are softened whereas the peak position of CuO_2 planar oxygen mode stays unchanged showing that Sr is incorporated at the Ba sites. The excess conductivity analyses of conductivity data of these samples have shown an increase in the values of the phase relaxation time of the carriers τ_ϕ and the Fermi velocity v_F of superconducting carriers with the doping of Sr in the final compound. The $V_F = \frac{\pi\xi_C\Delta}{\hbar}$ depends on Fermi-vector $K_F = (3\pi^2 N/V)^{1/3}[n = N/V]$ which in turn depends on the density of the carriers. An increase in the values of v_F shows that the carrier's density in the superconducting CuO_2 planes is enhanced with the doping of Sr at the Ba sites despite an increase in the volume of the unit cell. It confirms that doped Sr atoms induce efficient transfer of the charge carriers to the conducting planes. The values of parameters such as $B_{c0}(T)$, $B_{c1}(T)$, and $J_c(0)$ are enhanced with the doping of Sr in the final compound. The values of these parameters crucially depend on the thermodynamic critical field B_c which is related to the free energy difference between the normal and superconducting electrons. The doped Sr at the Ba sites seems to promote an increase in the difference of free energy difference between normal and superconducting state and hence the values of these parameters. Moreover, the doped Sr atoms enhance the flux pinning characters that

can be witnessed in the decrease of London penetration depth $\lambda_{p.d}$ and the Ginzburg-Landau(GL) parameter κ.

References

1. Khan, N.A., Khurram, A.A.: Appl. Phys. Lett. **86**, 152502 (2005)
2. Khan, N.A., Husnain, G.: Phys. C **436**, 51 (2006)
3. Jassim, K.A., Alwan, T.J. J. Supercond. Nov. Magn. **22**, 861–865 (2009)
4. Liu, R.S., Chang, C.Y., Chen, J.M., Liu, R.G.: J. Supercond. **11**, 5 (1998)
5. Sekkina, M.M.A., Elsabawy, K.: J. Supercond.: Inc. Novel Magn. **4**, 15 (2002)
6. Toulemonde, P., Odier, P., Bordet, P., Le Floch, S., Suard, E.: J. Phys.: Condens. Matter. **16**, 4061–4076 (2004)
7. Yamada, N., Ido, M.: Phys. C **203**, 240–246 (1992)
8. Hickey, B.R., Du, Z.L., Xue, Y.Y., Ross, D.K., Dezaneti, L.M., Sun, Y.Y., Wu, N.L., Chu, C.W.: J. Phys. Chem. Solids **60**, 1655–1662 (1999)
9. Pansuria, K.M., Kuberkar, D.G., Baldha, G.J., Kulkarni, R.G.: J. Supercond. **10**, 1 (1997)
10. Wen, H.H., Mu, G., Fang, L., Yang, H., Zhu, X.: Lett. J. Exploring Front. Phys. **82**, 17009 (2008)
11. Gao a, W.B., Liu a, Q.Q., Yang a, L.X., Yua, Y., Li a, F.Y., Wanga, X.C., Zhu a, J.L., Jin a, C.Q., Uchida, S.: Phys. C **470**, S19-S20 (2010)
12. Sekkina, M.M.A., Elsabawy, K.M.: Phys, C **377**, 254–259 (2002)
13. Gao, W.B., Liu, Q.Q., Yang, L.X., Yu, Y., Li, F.Y., Wang, X.C., Zhu, J.L., Jin, C.Q., Uchida, S.: Phys. C **470**, S19–S20 (2010)
14. Sato, T., Nakane, H., Mori, N., Yoshizawa, S.: Phys. C **344-360**, 244–247 (2003)
15. Manmeet Kaur, R., Srinibasan, G.K., Mehta, D., Kanjilal, R., Pinto, S.B., Ogale, S., Ganesan, M.V.: Phys. C **443**, 61–68 (2006)
16. Lawrence, W.E., Doniach, S. In: Kanda, E. (ed.): Proceedings of the twelfth international conference on low temperature physics, p. 361, Keigaku, Tokyo (1971)
17. Abu Aly, A.I., Ibrahim, I.H., Awad, R.A., El-Harizy, A.: J. Supercond. Nov. Magn. **23**, 1325 (2010)
18. Rojas Sarmiento, M.P., Uribe Laverde, M.A., Vera Lopez, E., Landinez Tellez, D.A., Roa-Rojas, J.: Phys. B **398**, 360 (2007)
19. Ben Azzouz, F., Zouaoui, M., Annabi, M., Ben Salem, M.: Sol. Stat. Phys. (C) **3**, 3048 (2006)
20. Solovjov, A.L., Dmitriev, V.M., Habermeier, H.-U.: Phys. Rev. B **55**, 8551 (1997)